

Query-Efficient Hard-label Black-box Attack: An Optimization-based Approach

Minhao Cheng¹, Thong Le¹, Pin-Yu Chen³, Jinfeng Yi², Huan Zhang¹, Cho-Jui Hsieh¹

¹Department of Computer Science, University of California, Davis, CA 95616

²JD AI Research, Beijing, China

³IBM Research, Yorktown Heights, NY 10598

mhcheng@ucdavis.edu, thmle@ucdavis.edu, pin-yu.chen@ibm.com, yijinfeng@jd.com,
echezhang@ucdavis.edu, chohsieh@ucdavis.edu

Abstract

We study the problem of attacking a machine learning model in the *hard-label black-box* setting, where no model information is revealed except that the attacker can make queries to probe the corresponding hard-label decisions. This is a very challenging problem since the direct extension of state-of-the-art white-box attacks (e.g., C&W or PGD) to the hard-label black-box setting will require minimizing a non-continuous step function, which is combinatorial and cannot be solved by a gradient-based optimizer. The only current approach is based on random walk on the boundary [1], which requires lots of queries and lacks convergence guarantees. We propose a novel way to formulate the hard-label black-box attack as a real-valued optimization problem which is usually continuous and can be solved by any zeroth order optimization algorithm. For example, using the Randomized Gradient-Free method [2], we are able to bound the number of iterations needed for our algorithm to achieve stationary points. We demonstrate that our proposed method outperforms the previous random walk approach to attacking convolutional neural networks on MNIST, CIFAR, and ImageNet datasets. More interestingly, we show that the proposed algorithm can also be used to attack other discrete and non-continuous machine learning models, such as Gradient Boosting Decision Trees (GBDT).

1 Introduction

It has been observed recently that machine learning algorithms, especially deep neural networks, are vulnerable to adversarial examples [3, 4, 5, 6, 7, 8]. For example, in image classification problems, attack algorithms [9, 3, 10] can find adversarial examples for almost every image with very small human-imperceptible perturbation. The problem of finding an adversarial example can be posed as solving an optimization problem—within a small neighbourhood around the original example, find a point to optimize the cost function measuring the “successfulness” of an attack. Solving this objective function with gradient-based optimizer leads to state-of-the-art attacks [9, 3, 10, 4, 11].

Most current attacks [3, 9, 4, 12] consider the “white-box” setting, where the machine learning model is fully exposed to the attacker. In this setting, the gradient of the above-mentioned attack objective function can be computed by back-propagation, so attacks can be done very easily. This white-box setting is clearly unrealistic when the model parameters are unknown to an attacker. Instead, several recent works consider the “score-based black-box” setting, where the machine learning model is unknown to the attacker, but it is possible to make queries to obtain the corresponding probability outputs of the model [10, 13]. However, in many cases real-world models will not provide probability outputs to users. Instead, only the final decision (e.g., top-1 predicted class) can be observed. It is therefore interesting to show whether machine learning model is vulnerable in this setting.

Furthermore, existing gradient-based attacks cannot be applied to some non-continuous machine learning models which involve discrete decisions. For example, the robustness of decision-tree based models (random forest and gradient boosting decision trees (GBDT)) cannot be evaluated using gradient-based approaches, since the gradient of these functions does not exist.

In this paper, we develop an optimization-based framework for attacking machine learning models in a more realistic and general “hard-label black-box” setting. We assume that the model is not revealed and the attacker can only make queries to get the corresponding **hard-label decision** instead of the probability outputs (also known as soft labels).

Attacking in this setting is very challenging and almost all the previous attacks fail due to the following two reasons. First, the gradient cannot be computed directly by backpropagation, and finite differences based approaches also fail because the hard-label output is insensitive to small input perturbations; second, since only hard-label decision is observed, the attack objective functions become discontinuous with discrete outputs, which is combinatorial in nature and hard to optimize (see Section 2.4 for more details).

In this paper, we make hard-label black-box attacks possible and query-efficient by reformulating the attack as a novel real-valued optimization problem, which is usually continuous and much easier to solve. Although the objective function of this reformulation cannot be written in an analytical form, we show how to use model queries to evaluate its function value and apply any zeroth order optimization algorithm to solve it. Furthermore, we prove that by carefully controlling the numerical accuracy of function evaluations, a Random Gradient-Free (RGF) method can converge to stationary points as long as the boundary is smooth. We note that this is the first attack with a guaranteed convergence rate in the hard-label black-box setting. In the experiments, we show our algorithm can be successfully used to attack hard-label black-box CNN models on MNIST, CIFAR, and ImageNet with far less number of queries compared to the state-of-art algorithm.

Moreover, since our algorithm does not depend on the gradient of the classifier, we can apply our approach to other non-differentiable classifiers besides neural networks. We show an interesting application in attacking Gradient Boosting Decision Tree, which cannot be attacked by all the existing gradient-based methods even in the white-box setting. Our method can successfully find adversarial examples with imperceptible perturbations for a GBDT within 30,000 queries.

2 Background and Related work

We will first introduce our problem setting and give a brief literature review to highlight the difficulty of attacking hard-label black-box models.

2.1 Problem Setting

For simplicity, we consider attacking a K -way multi-class classification model in this paper. Given the classification model $f : \mathbb{R}^d \rightarrow \{1, \dots, K\}$ and an original example \mathbf{x}_0 , the goal is to generate an adversarial example \mathbf{x} such that

$$\mathbf{x} \text{ is close to } \mathbf{x}_0 \quad \text{and} \quad f(\mathbf{x}) \neq f(\mathbf{x}_0) \quad (\mathbf{x} \text{ is misclassified by model } f.) \quad (1)$$

2.2 White-box attacks

Most attack algorithms in the literature consider the white-box setting, where the classifier f is exposed to the attacker. For neural networks, under this assumption, back-propagation can be conducted on the target model because both network structure and weights are known by the attacker. For classification models in neural networks, it is usually assumed that $f(\mathbf{x}) = \operatorname{argmax}_i (Z(\mathbf{x})_i)$, where $Z(\mathbf{x}) \in \mathbb{R}^K$ is the final (logit) layer output, and $Z(\mathbf{x})_i$ is the prediction score for the i -th class. The objectives in (1) can then be naturally formulated as the following optimization problem:

$$\operatorname{argmin}_{\mathbf{x}} \{ \operatorname{Dis}(\mathbf{x}, \mathbf{x}_0) + c\mathcal{L}(Z(\mathbf{x})) \} := h(\mathbf{x}), \quad (2)$$

where $\operatorname{Dis}(\cdot, \cdot)$ is some distance measurement (e.g., ℓ_2 , ℓ_1 or ℓ_∞ norm in Euclidean space), $\mathcal{L}(\cdot)$ is the loss function corresponding to the goal of the attack, and c is a balancing parameter. For *untargeted attack*, where the goal is to make the target classifier misclassify, the loss function can be defined as

$$\mathcal{L}(Z(\mathbf{x})) = \max\{ [Z(\mathbf{x})]_{y_0} - \max_{i \neq y_0} [Z(\mathbf{x})]_i, -\kappa \}, \quad (3)$$

where y_0 is the original label predicted by the classifier. For *targeted attack*, where the goal is to turn it into a specific target class t , the loss function can also be defined accordingly.

Therefore, attacking a machine learning model can be posed as solving this optimization problem [9, 12], which is also known as the C&W attack or the EAD attack depending on the choice of the distance measurement. To solve (2), one can apply any gradient-based optimization algorithm such as SGD or Adam, since the gradient of $\mathcal{L}(Z(\mathbf{x}))$ can be computed via back-propagation.

The ability of computing gradient also enables many different attacks in the white-box setting. For example, eq (2) can also be turned into a constrained optimization problem, which can then be solved by projected gradient descent (PGD) [11]. FGSM [3] is the special case of one step PGD with ℓ_∞ norm distance. Other algorithms such as Deepfool [6] also solve similar optimization problems to construct adversarial examples.

2.3 Previous work on black-box attack

In real-world systems, usually the underlying machine learning model will not be revealed and thus white-box attacks cannot be applied. This motivates the study of attacking machine learning models in the *black-box setting*, where attackers do not have any information about the function f . And the only valid operation is to make queries to the model and get the corresponding output $f(\mathbf{x})$. The first approach for black-box attack is using transfer attack [14]—instead of attacking the original model f , attackers try to construct a substitute model \hat{f} to mimic f and then attack \hat{f} using white-box attack methods. This approach has been well studied and analyzed in [15]. However, recent papers have shown that attacking the substitute model usually leads to much larger distortion and low success rate [10]. Therefore, instead, [10] considers the *score-based* black-box setting, where attackers can use \mathbf{x} to query the softmax layer output in addition to the final classification result. In this case, they can reconstruct the loss function (3) and evaluate it as long as the objective function $h(\mathbf{x})$ exists for any \mathbf{x} . Thus a zeroth order optimization approach can be directly applied to minimize $h(\mathbf{x})$. [16] further improves the query complexity of [10] by introducing two novel building blocks: (i) an adaptive random gradient estimation algorithm that balances query counts and distortion, and (ii) a well-trained autoencoder that achieves attack acceleration. [13] also solves a score-based attack problem using an evolutionary algorithm and it shows their method could be applied to hard-label black-box setting as well.

2.4 Difficulty of hard-label black-box attacks

Throughout this paper, the hard-label black-box setting refers to cases where real-world ML systems only provide limited prediction results of an input query. Specifically, only the final decision (top-1 predicted label) instead of probability outputs is known to an attacker.

Attacking in this setting is very challenging. In Figure 1a, we show a simple 3-layer neural network’s decision boundary. Note that the $\mathcal{L}(Z(\mathbf{x}))$ term is continuous as in Figure 1b because the logit layer output is real-valued functions. However, in the hard-label black-box setting, only $f(\cdot)$ is available instead of $Z(\cdot)$. Since $f(\cdot)$ can only be one-hot vector, if we plug-in f into the loss function, $\mathcal{L}(f(\mathbf{x}))$ (as shown in Figure 1c) will be discontinuous and with discrete outputs.

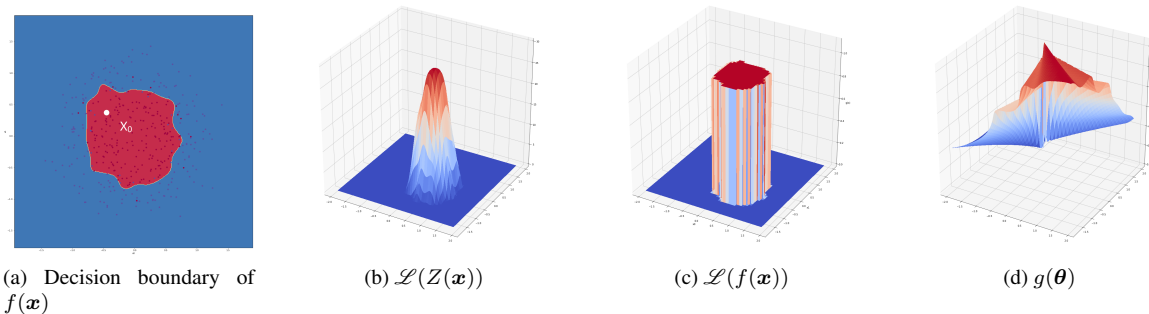


Figure 1: (a) A neural network classifier. (b) illustrates the loss function of C&W attack, which is continuous and hence can be easily optimized. (c) is the C&W loss function in the hard-label setting, which is discrete and discontinuous. (d) our proposed attack objective $g(\theta)$ for this problem, which is continuous and easier to optimize. See detailed discussions in Section 3.

Optimizing this function will require combinatorial optimization or search algorithms, which is almost impossible to do given high dimensionality of the problem. Therefore, almost no algorithm can successfully conduct hard-label black-box attack in the literature. The only current approach [1] is based on random-walk on the boundary. Although this decision-based attack can find adversarial examples with comparable distortion with white-box attacks, it suffers from

exponential search time, resulting in lots of queries, and lacks convergence guarantees. We show that our optimization-based algorithm can significantly reduce the number of queries compared with decision-based attack, and has guaranteed convergence in the number of iterations (queries).

3 Algorithms

Now we will introduce a novel way to re-formulate hard-label black-box attack as another optimization problem, show how to evaluate the function value using hard-label queries, and then apply a zeroth order optimization algorithm to solve it.

3.1 A Boundary-based Re-formulation

For a given example x_0 , true label y_0 and the hard-label black-box function $f : \mathbb{R}^d \rightarrow \{1, \dots, K\}$, we define our objective function $g : \mathbb{R}^d \rightarrow \mathbb{R}$ depending on the type of attack:

$$\text{Untargeted attack: } g(\theta) = \operatorname{argmin}_{\lambda > 0} \left(f(x_0 + \lambda \frac{\theta}{\|\theta\|}) \neq y_0 \right) \quad (4)$$

$$\text{Targeted attack (given target } t): g(\theta) = \operatorname{argmin}_{\lambda > 0} \left(f(x_0 + \lambda \frac{\theta}{\|\theta\|}) = t \right). \quad (5)$$

In this formulation, θ represents the search direction and $g(\theta)$ is the distance from x_0 to the nearest adversarial example along the direction θ . The difference between (4) and (5) corresponds to the different definitions of “successfulness” in untargeted and targeted attack, where the former one aims to turn the prediction into any incorrect label and the later one aims to turn the prediction into the target label. For untargeted attack, $g(\theta)$ also corresponds to the distance to the decision boundary along the direction θ . In image problems the input domain of f is bounded, so we will add corresponding upper/lower bounds in the definition of (4) and (5).

Instead of searching for an adversarial example, we search the direction θ to minimize the distortion $g(\theta)$, which leads to the following optimization problem:

$$\min_{\theta} g(\theta). \quad (6)$$

Finally, the adversarial example can be found by $x^* = x_0 + g(\theta^*) \frac{\theta^*}{\|\theta^*\|}$, where θ^* is the optimal solution of (6).

Note that unlike the C&W or PGD objective functions, which are discontinuous step functions in the hard-label setting (see Section 2), $g(\theta)$ maps input direction to real-valued output (distance to decision boundary), which is usually continuous—a small change of θ usually leads to a small change of $g(\theta)$, as can be seen from Figure 2.

Moreover, we give three examples of $f(x)$ defined in two dimension input space and their corresponding $g(\theta)$. In Figure 3a, we have a continuous classification function defined as follows

$$f(x) = \begin{cases} 1, & \text{if } \|x\|^2 \geq 0.4 \\ 0, & \text{otherwise.} \end{cases}$$

In this case, as shown in Figure 3c, $g(\theta)$ is continuous. Moreover, in Figure 3b and Figure 1a, we show decision boundaries generated by GBDT and neural network classifier, which are not continuous. However, as showed in Figure 3d and Figure 1d, even if the classifier function is not continuous, $g(\theta)$ is still continuous. This makes it easy to apply zeroth order method to solve (6).

Compute $g(\theta)$ up to certain accuracy. We are not able to evaluate the gradient of g , but we can evaluate the function value of g using the hard-label queries to the original function f . For simplicity, we focus on untargeted attack here, but the same procedure can be applied to targeted attack as well.

First, we discuss how to compute $g(\theta)$ directly without additional information. This is used in the initialization step of our algorithm. For a given normalized θ , we do a fine-grained search and then a binary search. In fine-grained search,

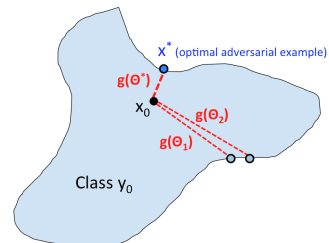


Figure 2: Illustration

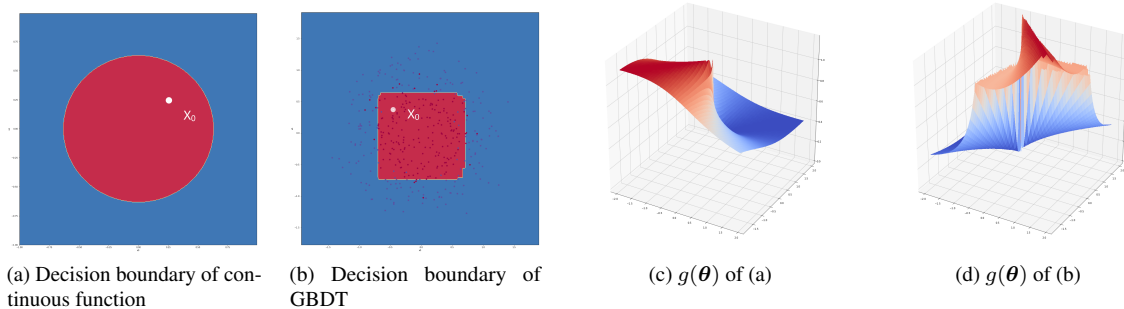


Figure 3: Examples of decision boundary of classification function $f(\mathbf{x})$ and corresponding $g(\boldsymbol{\theta})$

we query the points $\{\mathbf{x}_0 + \alpha\boldsymbol{\theta}, \mathbf{x}_0 + 2\alpha\boldsymbol{\theta}, \dots\}$ one by one until we find $f(\mathbf{x} + i\alpha\boldsymbol{\theta}) \neq y_0$. This means the boundary goes between $[\mathbf{x}_0 + (i-1)\alpha\boldsymbol{\theta}, \mathbf{x}_0 + i\alpha\boldsymbol{\theta}]$. We then enter the second phase and conduct a binary search to find the solution within this region (same with line 11–17 in Algorithm 1). Note that there is an upper bound of the first stage if we choose $\boldsymbol{\theta}$ by the direction of $\mathbf{x} - \mathbf{x}_0$ with some \mathbf{x} from another class. This procedure is used to find the initial $\boldsymbol{\theta}_0$ and corresponding $g(\boldsymbol{\theta}_0)$ in our optimization algorithm. We omit the detailed algorithm for this part since it is similar to Algorithm 1.

Next, we discuss how to compute $g(\boldsymbol{\theta})$ when we know the solution is very close to a value v . This is used in all the function evaluations in our optimization algorithm, since the current solution is usually close to the previous solution, and when we estimate the gradient using (7), the queried direction will only be a small perturbation of the previous one. In this case, we first increase or decrease v in local region to find the interval that contains boundary (e.g. $f(v) = y_0$ and $f(v') \neq y_0$), then conduct a binary search to find the final value of g . Our procedure for computing g value is presented in Algorithm 1.

Algorithm 1 Compute $g(\boldsymbol{\theta})$ locally

```

1: Input: Hard-label model  $f$ , original image  $x_0$ , query direction  $\boldsymbol{\theta}$ , previous value  $v$ , increase/decrease ratio
    $\alpha = 0.01$ , stopping tolerance  $\epsilon$  (maximum tolerance of computed error)
2:  $\boldsymbol{\theta} \leftarrow \boldsymbol{\theta} / \|\boldsymbol{\theta}\|$ 
3: if  $f(\mathbf{x}_0 + v\boldsymbol{\theta}) = y_0$  then
4:    $v_{left} \leftarrow v, v_{right} \leftarrow (1 + \alpha)v$ 
5:   while  $f(\mathbf{x}_0 + v_{right}\boldsymbol{\theta}) = y_0$  do
6:      $v_{right} \leftarrow (1 + \alpha)v_{right}$ 
7: else
8:    $v_{right} \leftarrow v, v_{left} \leftarrow (1 - \alpha)v$ 
9:   while  $f(\mathbf{x}_0 + v_{left}\boldsymbol{\theta}) \neq y_0$  do
10:     $v_{left} \leftarrow (1 - \alpha)v_{left}$ 
11: ## Binary Search within  $[v_{left}, v_{right}]$ 
12: while  $v_{right} - v_{left} > \epsilon$  do
13:    $v_{mid} \leftarrow (v_{right} + v_{left})/2$ 
14:   if  $f(\mathbf{x}_0 + v_{mid}\boldsymbol{\theta}) = y_0$  then
15:      $v_{left} \leftarrow v_{mid}$ 
16:   else
17:      $v_{right} \leftarrow v_{mid}$ 
18: return  $v_{right}$ 

```

3.2 Zeroth Order Optimization

To solve the optimization problem (1) for which we can only evaluate function value instead of gradient, zeroth order optimization algorithms can be naturally applied. In fact, after the reformulation, the problem can be potentially solved by any zeroth order optimization algorithm, like zeroth order gradient descent or coordinate descent (see [17] for a comprehensive survey).

Here we propose to solve (1) using Randomized Gradient-Free (RGF) method proposed in [2, 18]. In practice we found it outperforms zeroth-order coordinate descent. In each iteration, the gradient is estimated by

$$\hat{\mathbf{g}} = \frac{g(\boldsymbol{\theta} + \beta \mathbf{u}) - g(\boldsymbol{\theta})}{\beta} \cdot \mathbf{u} \quad (7)$$

where \mathbf{u} is a random Gaussian vector, and $\beta > 0$ is a smoothing parameter (we set $\beta = 0.005$ in all our experiments). The solution is then updated by $\boldsymbol{\theta} \leftarrow \boldsymbol{\theta} - \eta \hat{\mathbf{g}}$ with a step size η . The procedure is summarized in Algorithm 2.

Algorithm 2 RGF for hard-label black-box attack

- 1: **Input:** Hard-label model f , original image x_0 , initial $\boldsymbol{\theta}_0$.
 - 2: **for** $t = 0, 1, 2, \dots, T$ **do**
 - 3: Randomly choose \mathbf{u}_t from a zero-mean Gaussian distribution
 - 4: Evaluate $g(\boldsymbol{\theta}_t)$ and $g(\boldsymbol{\theta}_t + \beta \mathbf{u})$ using Algorithm 1
 - 5: Compute $\hat{\mathbf{g}} = \frac{g(\boldsymbol{\theta}_t + \beta \mathbf{u}) - g(\boldsymbol{\theta}_t)}{\beta} \cdot \mathbf{u}$
 - 6: Update $\boldsymbol{\theta}_{t+1} = \boldsymbol{\theta}_t - \eta_t \hat{\mathbf{g}}$
 - 7: **return** $x_0 + g(\boldsymbol{\theta}_T) \boldsymbol{\theta}_T$
-

There are several implementation details when we apply this algorithm. First, for high-dimensional problems, we found the estimation in (7) is very noisy. Therefore, instead of using one vector, we sample q vectors from Gaussian distribution and average their estimators to get $\hat{\mathbf{g}}$. We set $q = 20$ in all the experiments. The convergence proofs can be naturally extended to this case. Second, instead of using a fixed step size (suggested in theory), we use a backtracking line-search approach to find step size at each step. This leads to additional query counts, but makes the algorithm more stable and eliminates the need to hand-tuning the step size.

3.3 Theoretical Analysis

If $g(\boldsymbol{\theta})$ can be computed exactly, it has been proved in [2] that RGF in Algorithm 2 requires at most $O(\frac{d}{\delta^2})$ iterations to converge to a point with $\|\nabla g(\boldsymbol{\theta})\|^2 \leq \delta^2$. However, in our algorithm the function value $g(\boldsymbol{\theta})$ cannot be computed exactly; instead, we compute it up to ϵ -precision, and this precision can be controlled by binary threshold in Algorithm 1. We thus extend the proof in [2] to include the case of approximate function value evaluation, as described in the following theorem.

Theorem 1 *In Algorithm 2, suppose g has Lipschitz-continuous gradient with constant $L_1(g)$. If the error of function value evaluation is controlled by $\epsilon \sim O(\beta \delta^2)$ and $\beta \leq O(\frac{\delta}{d L_1(g)})$, then in order to obtain $\frac{1}{N+1} \sum_{k=0}^N E_{\mathcal{U}_k} (\|\nabla g(\boldsymbol{\theta}_k)\|^2) \leq \delta^2$, the total number of iterations is at most $O(\frac{d}{\delta^2})$.*

Detailed proofs can be found in the appendix. Note that the binary search procedure could obtain the desired function value precision in $O(\log \delta)$ steps. By using the same idea with Theorem 1 and following the proof in [2], we could also achieve $O(\frac{d^2}{\delta^3})$ complexity when $g(\boldsymbol{\theta})$ is non-smooth but Lipschitz continuous.

4 Experimental results

We test the performance of our hard-label black-box attack algorithm on convolutional neural network (CNN) models and compare with decision-based attack [1]. Furthermore, we show our method can be applied to attack Gradient Boosting Decision Tree (GBDT) and present some interesting findings.

Table 1: Results of untargeted attack.

	MNIST		CIFAR10		Imagenet (ResNet-50)	
	Avg L_2	# queries	Avg L_2	# queries	Avg L_2	# queries
Decision-attack (black-box)	1.1222	60,293	0.1575	123,879	5.9791	123,407
	1.1087	143,357	0.1501	220,144	3.7725	260,797
Opt-attack (black-box)	1.188	22,940	0.2050	40,941	6.9796	71,100
	1.049	51,683	0.1625	77,327	4.7100	127,086
	1.011	126,486	0.1451	133,662	3.1120	237,342
C&W (white-box)	0.9921	-	0.1012	-	1.9365	-

4.1 Attack CNN image classification models

We use three standard datasets: MNIST [19], CIFAR-10 [20] and ImageNet-1000 [21]. To have a fair comparison with previous work, we adopt the same networks used in both [9] and [1]. In detail, both MNIST and CIFAR use the same network structure with four convolution layers, two max-pooling layers and two fully-connected layers. Using the parameters provided by [9], we could achieve 99.5% accuracy on MNIST and 82.5% accuracy on CIFAR-10, which is similar to what was reported in [9]. For Imagenet-1000, we use the pretrained network Resnet-50 [22] provided by torchvision¹, which could achieve 76.15% top-1 accuracy. All models are trained using Pytorch and our source code is publicly available².

We include the following algorithms into comparison:

- Opt-based black-box attack (Opt-attack): our proposed algorithm.
- Decision-based black-box attack [1] (Decision-attack): the only previous work on attacking hard-label black box model. We use the authors’ implementation and use default parameters provided in Foolbox³.
- C&W white-box attack [9]: one of the current state-of-the-art attacking algorithm in the white-box setting. We do binary search on parameter c per image to achieve the best performance. Attacking in the white-box setting is a much easier problem, so we include C&W attack just for reference and indicate the best performance we can possibly achieve.

For all the cases, we conduct adversarial attacks for randomly sampled $N = 100$ images from validation sets. Note that all three attacks have 100% successful rate, and we report the average L_2 distortion, defined by $\frac{1}{N} \sum_{i=1}^N \|\mathbf{x}^{(i)} - \mathbf{x}_0^{(i)}\|_2$, where $\mathbf{x}^{(i)}$ is the adversarial example constructed by an attack algorithm and $\mathbf{x}_0^{(i)}$ is the original i -th example. For black-box attack algorithms, we also report average number of queries for comparison.

4.1.1 Untargeted Attack

For untargeted attack, the goal is to turn a correctly classified image into any other label. The results are presented in Table 1. Note that for both Opt-attack and Decision-attack, by changing stopping conditions we can get the performance with different number of queries.

First, we compare two black-box attack methods in Table 1. Our algorithm consistently achieves smaller distortion with less number of queries than Decision-attack. For example, on MNIST data, we are able to reduce the number of queries by 3-4 folds, and Decision-attack converges to worse solutions in all the 3 datasets. Compared with C&W attack, we found black-box attacks attain slightly worse distortion on MNIST and CIFAR. This is reasonable because white-box attack has much more information than black-box attack and is strictly easier. We note that the experiments in [1] conclude that C&W

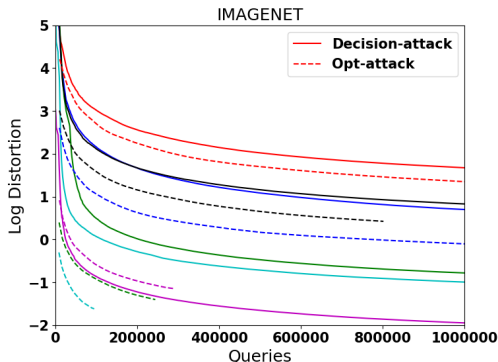


Figure 4: Log distortion comparison of Decision-attack (solid curves) vs Opt-attack (dotted curves) over number of queries for 6 different images.

¹<https://github.com/pytorch/vision/tree/master/torchvision>

²<https://github.com/LeMinhThong/blackbox-attack>

³<https://github.com/bethgelab/foolbox>

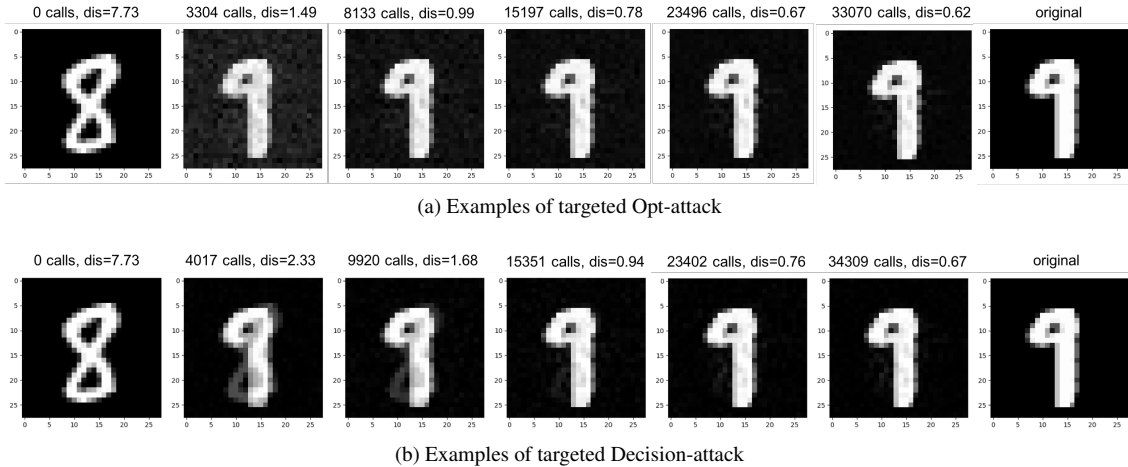


Figure 5: Example quality comparison between targeted Opt-attack and Decision-attack. Opt-attack can achieve a better result with less queries.

Table 2: Results of targeted attack.

	MNIST		CIFAR10	
	Avg L_2	# queries	Avg L_2	# queries
Decision-attack (black-box)	2.3158	30,103	0.2850	55,552
	2.0052	58,508	0.2213	140,572
	1.8668	192,018	0.2122	316,791
Opt-attack (black-box)	1.8522	46,248	0.2758	61,869
	1.7744	57,741	0.2369	141,437
	1.7114	73,293	0.2300	186,753
C&W (white-box)	1.4178	-	0.1901	-

and Decision-attack have similar performance because they only run C&W with a single regularization parameter c without doing binary search to obtain the optimal parameter. For ImageNet, since we constraint the number of queries, the distortion of black-box attacks is much worse than C&W attack. The gap can be reduced by increasing the number of queries as showed in Figure 4.

4.1.2 Targeted attack

The results for targeted attack is presented in Table 2. Following the experiments in [1], for each randomly sampled image with label i we set target label $t = (i + 1)$ module 10. On MNIST data, we found our algorithm is more than 4 times faster (in terms of number of queries) than Decision-attack and converge to a better solution. On CIFAR data, our algorithm has similar efficiency with Decision-attack at the first 60,000 queries, but converges to a slightly worse solution. Also, we show a example quality comparison from the same starting point to the original sample in Figure 5.

4.1.3 Attack Gradient Boosting Decision Tree (GBDT)

To evaluate our method’s ability to attack models with discrete decision functions, we conduct our untargeted attack on gradient booting decision tree (GBDT). In this experiment, we use two standard datasets: HIGGS [23] for binary classification and MNIST [19] for multi-class classification. We use popular LightGBM⁴ framework to train the GBDT models. Using suggested parameters⁵, we could achieve 0.8457 AUC for HIGGS and 98.09% accuracy for MNIST. The results of untargeted attack on GBDT are in Table 3.

⁴<https://github.com/Microsoft/LightGBM>

⁵https://github.com/Koziev/MNIST_Boosting

Table 3: Results of untargeted attack on gradient boosting decision tree.

	HIGGS		MNIST	
	Avg L_2	# queries	Avg L_2	# queries
	0.3458	4,229	0.6113	5,125
Ours	0.2179	11,139	0.5576	11,858
	0.1704	29,598	0.5505	32,230

As shown in Table 3, by using around 30K queries, we could get a small distortion on both datasets, which firstly uncovers the vulnerability of GBDT models. Tree-based methods are well-known for its good interpretability. And because of that, they are widely used in the industry. However, we show that even with good interpretability and a similar prediction accuracy with convolution neural network, the GBDT models are vulnerable under our Opt-attack. This result raises a question about tree-based models’ robustness, which will be an interesting direction in the future.

5 Conclusion

In this paper, we propose a generic and optimization-based hard-label black-box attack algorithm, which can be applied to discrete and non-continuous models other than neural networks, such as the gradient boosting decision tree. Our method enjoys query-efficiency and has a theoretical convergence guarantee on the attack performance. Moreover, our attack achieves smaller or similar distortion using 3-4 times less queries compared with the state-of-the-art algorithm.

References

- [1] Wieland Brendel, Jonas Rauber, and Matthias Bethge. Decision-based adversarial attacks: Reliable attacks against black-box machine learning models. *arXiv preprint arXiv:1712.04248*, 2017.
- [2] Yurii Nesterov and Vladimir Spokoiny. Random gradient-free minimization of convex functions. *Foundations of Computational Mathematics*, 17(2):527–566, 2017.
- [3] Ian J Goodfellow, Jonathon Shlens, and Christian Szegedy. Explaining and harnessing adversarial examples. *arXiv preprint arXiv:1412.6572*, 2014.
- [4] Christian Szegedy, Wojciech Zaremba, Ilya Sutskever, Joan Bruna, Dumitru Erhan, Ian Goodfellow, and Rob Fergus. Intriguing properties of neural networks. *arXiv preprint arXiv:1312.6199*, 2013.
- [5] Seyed-Mohsen Moosavi-Dezfooli, Alhussein Fawzi, Omar Fawzi, and Pascal Frossard. Universal adversarial perturbations.
- [6] Seyed Mohsen Moosavi Dezfooli, Alhussein Fawzi, and Pascal Frossard. Deepfool: a simple and accurate method to fool deep neural networks. In *Proceedings of 2016 IEEE Conference on Computer Vision and Pattern Recognition (CVPR)*, number EPFL-CONF-218057, 2016.
- [7] Hongge Chen, Huan Zhang, Pin-Yu Chen, Jinfeng Yi, and Cho-Jui Hsieh. Attacking visual language grounding with adversarial examples: A case study on neural image captioning. In *ACL*, 2018.
- [8] Minhao Cheng, Jinfeng Yi, Huan Zhang, Pin-Yu Chen, and Cho-Jui Hsieh. Seq2sick: Evaluating the robustness of sequence-to-sequence models with adversarial examples. *CoRR*, 2018.
- [9] Nicholas Carlini and David Wagner. Towards evaluating the robustness of neural networks. In *Security and Privacy (SP), 2017 IEEE Symposium on*, pages 39–57. IEEE, 2017.
- [10] Pin-Yu Chen, Huan Zhang, Yash Sharma, Jinfeng Yi, and Cho-Jui Hsieh. Zoo: Zeroth order optimization based black-box attacks to deep neural networks without training substitute models. In *Proceedings of the 10th ACM Workshop on Artificial Intelligence and Security*, pages 15–26. ACM, 2017.

- [11] Aleksander Madry, Aleksandar Makelov, Ludwig Schmidt, Dimitris Tsipras, and Adrian Vladu. Towards deep learning models resistant to adversarial attacks. In *ICLR*, 2018.
- [12] Pin-Yu Chen, Yash Sharma, Huan Zhang, Jinfeng Yi, and Cho-Jui Hsieh. Ead: elastic-net attacks to deep neural networks via adversarial examples. In *AAAI*, 2018.
- [13] Andrew Ilyas, Logan Engstrom, Anish Athalye, and Jessy Lin. Query-efficient black-box adversarial examples. *arXiv preprint arXiv:1712.07113*, 2017.
- [14] Nicolas Papernot, Patrick McDaniel, Ian Goodfellow, Somesh Jha, Z Berkay Celik, and Ananthram Swami. Practical black-box attacks against machine learning. In *Proceedings of the 2017 ACM on Asia Conference on Computer and Communications Security*, pages 506–519. ACM, 2017.
- [15] Arjun Nitin Bhagoji, Warren He, Bo Li, and Dawn Song. Exploring the space of black-box attacks on deep neural networks. *arXiv preprint arXiv:1712.09491*, 2017.
- [16] Chun-Chen Tu, Pai-Shun Ting, Pin-Yu Chen, Sijia Liu, Huan Zhang, Jinfeng Yi, Cho-Jui Hsieh, and Shin-Ming Cheng. Autozoom: Autoencoder-based zeroth order optimization method for attacking black-box neural networks. *CoRR*, abs/1805.11770, 2018.
- [17] Andrew R Conn, Katya Scheinberg, and Luis N Vicente. *Introduction to derivative-free optimization*, volume 8. Siam, 2009.
- [18] Saeed Ghadimi and Guanghui Lan. Stochastic first-and zeroth-order methods for nonconvex stochastic programming. *SIAM Journal on Optimization*, 23(4):2341–2368, 2013.
- [19] Yann LeCun, Léon Bottou, Yoshua Bengio, and Patrick Haffner. Gradient-based learning applied to document recognition. *Proceedings of the IEEE*, 86(11):2278–2324, 1998.
- [20] Alex Krizhevsky. Learning multiple layers of features from tiny images. 2009.
- [21] Jia Deng, Wei Dong, Richard Socher, Li-Jia Li, Kai Li, and Li Fei-Fei. Imagenet: A large-scale hierarchical image database. In *Computer Vision and Pattern Recognition, 2009. CVPR 2009. IEEE Conference on*, pages 248–255. IEEE, 2009.
- [22] Kaiming He, Xiangyu Zhang, Shaoqing Ren, and Jian Sun. Deep residual learning for image recognition. In *Proceedings of the IEEE conference on computer vision and pattern recognition*, pages 770–778, 2016.
- [23] Pierre Baldi, Peter Sadowski, and Daniel Whiteson. Searching for exotic particles in high-energy physics with deep learning. *Nature communications*, 5:4308, 2014.
- [24] Yurii Nesterov. Random gradient-free minimization of convex functions. Technical report, 2011.

6 Appendix

Because there is a stopping criterion in Algorithm 1, we couldn't achieve the exact $g(\boldsymbol{\theta})$. Instead, we could get \tilde{g} with ϵ error, i.e., $g(\boldsymbol{\theta}) - \epsilon \leq \tilde{g}(\boldsymbol{\theta}) \leq g(\boldsymbol{\theta}) + \epsilon$. Also, we define $\hat{g}(\boldsymbol{\theta}) = \frac{\tilde{g}(\boldsymbol{\theta} + \beta \mathbf{u}) - \tilde{g}(\boldsymbol{\theta})}{\beta} \cdot \mathbf{u}$ to be the noisy gradient estimator.

Following [24], we define the Gaussian smoothing approximation over $g(\boldsymbol{\theta})$, i.e.,

$$g_\beta(\boldsymbol{\theta}) = \frac{1}{\kappa} \int_E g(\boldsymbol{\theta} + \beta u) e^{-\frac{1}{2} \|u\|^2} du. \quad (8)$$

Also, we have the upper bounds for the moments $M_p = \frac{1}{\kappa} \int_E \|u\|^p e^{-\frac{1}{2} \|u\|^2} du$ from [24] Lemma 1.

For $p \in [0, 2]$, we have

$$M_p \leq d^{p/2}. \quad (9)$$

If $p \geq 2$, we have two-sided bounds

$$n^{p/2} \leq M_p \leq (p+n)^{p/2}. \quad (10)$$

6.1 Proof of Theorem 1

Suppose g has a Lipschitz-continuous gradient with constant $L_1(g)$, then

$$|g(y) - g(x) - \langle \nabla g(x), y - x \rangle| \leq \frac{1}{2} L_1(g) \|x - y\|^2. \quad (11)$$

We could bound $E_u(\|\hat{g}(\boldsymbol{\theta})\|^2)$ as follows. Since

$$\begin{aligned} (\tilde{g}(\boldsymbol{\theta} + \beta u)^2 - \tilde{g}(\boldsymbol{\theta})^2) &= [\tilde{g}(\boldsymbol{\theta} + \beta u) - \tilde{g}(\boldsymbol{\theta}) - \beta \langle \nabla g(\boldsymbol{\theta}), u \rangle + \beta \langle \nabla g(\boldsymbol{\theta}), u \rangle]^2 \\ &\leq 2(g(\boldsymbol{\theta} + \beta u) - g(\boldsymbol{\theta}) + \epsilon_{\boldsymbol{\theta} + \beta u} - \epsilon_{\boldsymbol{\theta}})^2 + 2\beta^2 \langle \nabla g(\boldsymbol{\theta}), u \rangle^2 \end{aligned} \quad (12)$$

and $|\epsilon_{\boldsymbol{\theta} + \beta u} - \epsilon_{\boldsymbol{\theta}}| \leq 2\epsilon$,

$$[\tilde{g}(\boldsymbol{\theta} + \beta u) - \tilde{g}(\boldsymbol{\theta})]^2 \leq 2\left(\frac{\beta}{2} L_1(g) \|u\|^2\right)^2 + 4\beta L_1(g) \|u\|^2 \epsilon + 8\epsilon^2 + 2\beta^2 \langle \nabla g(\boldsymbol{\theta}), u \rangle^2 \quad (13)$$

Take expectation over u , and with Theorem 3 in [24], which is $E_u(\|g'(\boldsymbol{\theta}, u) \cdot u\|^2) \leq (d+4) \|\nabla g(x)\|^2$,

$$\begin{aligned} E_u(\|\hat{g}(\boldsymbol{\theta})\|^2) &\leq \frac{\beta^2}{2} L_1^2(g) E_u(\|u\|^6) + 2E_u(\|g'(\boldsymbol{\theta}, u) \cdot u\|^2) + 4\beta^2 L_1(g) \epsilon E_u(\|u\|^4) + 8\epsilon^2 E_u(\|u\|^2) \\ &\leq \frac{\beta^2}{2} L_1^2(g) (d+6)^3 + 2(d+4) \|\nabla g(\boldsymbol{\theta})\|^2 + 4\beta \epsilon L_1(g) (d+4)^2 + 8\epsilon^2 d. \end{aligned} \quad (14)$$

With $\epsilon \sim O(\delta^2 \beta)$, we could bound $E_u(\|\tilde{g}(\boldsymbol{\theta})\|^2)$:

$$E_u(\|\hat{g}(\boldsymbol{\theta})\|^2) \leq \frac{\beta^2}{2} L_1^2(g) (d+6)^3 + 2(d+4) \|\nabla g(\boldsymbol{\theta})\|^2 + 4\beta^2 L_1(g) (d+4)^2 \delta^2 + 8\beta^2 d \delta^2. \quad (15)$$

We use the result that

$$\|\nabla g(\boldsymbol{\theta})\|^2 \leq 2\|\nabla g_\beta(\boldsymbol{\theta})\|^2 + \frac{\beta^2}{2} L_1^2(g) (d+4)^2, \quad (16)$$

which is proved in [24] Lemma 4.

Therefore, since $(n+6)^3 + 2(n+4)^3 \leq 3(n+5)^3$, we could get

$$\begin{aligned} E_u(\|\hat{g}(\boldsymbol{\theta})\|^2) &\leq \frac{\beta^2}{2} L_1^2(g) (d+6)^3 + 2(d+4) \|\nabla g(x)\|^2 + 2(d+4) \|\nabla g(\boldsymbol{\theta})\|^2 \\ &\quad + 4\beta^2 L_1(g) (d+4)^2 \delta^2 + 8\beta^2 d \delta^2 \\ &\leq \frac{\beta^2}{2} L_1^2(g) (d+6)^3 + 2(d+4) (2\|\nabla g_\beta(x)\|^2 + \frac{\beta^2}{2} L_1^2(g) (d+4)^2) \\ &\quad + 4\beta^2 L_1(g) (d+4)^2 \delta^2 + 8\beta^2 d \delta^2 \\ &\leq 4(d+4) \|\nabla g_\beta(x)\|^2 + \frac{3\beta^2}{2} L_1^2(g) (d+5)^3 + 4\beta^2 L_1(g) (d+4)^2 \delta^2 + 8\beta^2 d \delta^2 \end{aligned} \quad (17)$$

Therefore, since $g_\beta(\boldsymbol{\theta})$ has Lipschitz-continuous gradient:

$$|g_\beta(\boldsymbol{\theta}_{k+1}) - g_\beta(\boldsymbol{\theta}_k) + \alpha \langle \nabla g_\beta(\boldsymbol{\theta}_k), \hat{g}_\beta(\boldsymbol{\theta}_k) \rangle| \leq \frac{1}{2} \alpha^2 L_1(g_\beta) \|\hat{g}_\beta(\boldsymbol{\theta}_k)\|^2 \quad (18)$$

so that

$$g_\beta(\boldsymbol{\theta}_{k+1}) \leq g_\beta(\boldsymbol{\theta}_k) - \alpha \langle \nabla g_\beta(\boldsymbol{\theta}_k), \hat{g}_\beta(\boldsymbol{\theta}_k) \rangle + \frac{1}{2} \alpha^2 L_1(g_\beta) \|\hat{g}_\beta(\boldsymbol{\theta}_k)\|^2. \quad (19)$$

Since

$$\begin{aligned} E_u(\hat{g}(\boldsymbol{\theta}_k)) &= \frac{1}{\kappa} \int_E \frac{g(\boldsymbol{\theta} + \beta u) - g(\boldsymbol{\theta}) + \epsilon_{\boldsymbol{\theta} + \beta u} - \epsilon_{\boldsymbol{\theta}}}{\beta} u e^{-\frac{1}{2}\|u\|^2} du \\ &= \nabla g_\beta(\boldsymbol{\theta}_k) + \frac{1}{\kappa} \int_E \frac{\epsilon_{\boldsymbol{\theta} + \beta u} - \epsilon_{\boldsymbol{\theta}}}{\beta} u e^{-\frac{1}{2}\|u\|^2} du \\ &\leq \nabla g_\beta(\boldsymbol{\theta}_k) + \frac{2\epsilon}{\beta} n^{1/2} \cdot \mathbb{1} \end{aligned} \quad (20)$$

where $\mathbb{1}$ is a all-one vector, taking the expectation in u_k , we obtain

$$\begin{aligned} E_{u_k}(g_\beta(\boldsymbol{\theta}_{k+1})) &\leq g_\beta(\boldsymbol{\theta}_k) - \alpha_k \|\nabla g_\beta(\boldsymbol{\theta}_k)\|^2 + \alpha_k \langle \nabla g_\beta(\boldsymbol{\theta}_k), \frac{2\epsilon}{\beta} n^{1/2} \cdot \mathbb{1} \rangle + \frac{1}{2} \alpha_k^2 L_1(g_\beta) E_{u_k} \|\hat{g}_\beta(\boldsymbol{\theta}_k)\|^2 \\ E_{u_k}(g_\beta(\boldsymbol{\theta}_{k+1})) &\leq g_\beta(\boldsymbol{\theta}_k) - \alpha_k \|\nabla g_\beta(\boldsymbol{\theta}_k)\|^2 + \alpha_k \frac{2\epsilon}{\beta} n^{1/2} \|\nabla g_\beta(\boldsymbol{\theta}_k)\| \\ &\quad + \frac{1}{2} \alpha_k^2 L_1(g) (4(d+4) \|\nabla g_\beta(\boldsymbol{\theta}_k)\|^2 + \frac{3\beta^2}{2} L_1^2(g) (d+5)^3 + 4\beta^2 L_1(g) (d+4)^2 \delta^2 + 8\beta^2 d \delta^2). \end{aligned} \quad (21)$$

Choosing $\alpha_k = \hat{\alpha} = \frac{1}{4(d+4)L_1(f)}$, we obtain

$$\begin{aligned} E_{u_k}(g_\beta(\boldsymbol{\theta}_k + 1)) &\leq g_\beta(\boldsymbol{\theta}_k) - \frac{1}{2} \hat{\alpha} \|\nabla g_\beta(\boldsymbol{\theta}_k)\|^2 + \alpha_k \frac{2\epsilon}{\beta} d^{1/2} \|\nabla g_\beta(\boldsymbol{\theta}_k)\| + \frac{3\beta^2}{64} L_1(g) \frac{(d+5)^3}{(d+4)^2} \\ &\quad + \frac{\beta^2}{8} \delta^2 + \frac{\beta^2 d}{4(d+4)^2 L_1(g)} \delta^2. \end{aligned} \quad (22)$$

Since $(d+5)^3 \leq (d+8)(d+4)^2$, taking expectation over \mathcal{U}_k , where $\mathcal{U}_k = \{u_1, u_2, \dots, u_k\}$, we get

$$\phi_{k+1} \leq \phi_k - \frac{1}{2} \hat{\alpha} E_{\mathcal{U}_k} (\|\nabla g_\beta(\boldsymbol{\theta}_k)\|^2) + \frac{3\beta^2(d+8)}{64} L_1(g) + \frac{\beta^2}{8} \delta^2 + \frac{\beta^2 d}{4(d+4)^2 L_1(g)} \delta^2 + \hat{\alpha} d^{1/2} E_{\mathcal{U}_k} (\|\nabla g_\beta(\boldsymbol{\theta}_k)\|) \delta^2, \quad (23)$$

where $\phi_k = E_{\mathcal{U}_{k-1}}(g(\boldsymbol{\theta}_k))$, $k \geq 1$ and $\phi_0 = g(\boldsymbol{\theta}_0)$.

Assuming $g(x) \geq g^*$, summing over k and divided by $N+1$, we get

$$\begin{aligned} \frac{1}{N+1} \sum_{k=0}^N E_{\mathcal{U}_k} (\|\nabla g_\beta(\boldsymbol{\theta}_k)\|^2) &\leq 8(d+4) L_1(g) \left[\frac{g(x_0) - g^*}{N+1} + \frac{3\beta^2(d+8)}{16} L_1(g) + \frac{\beta^2}{8} \delta^2 \right. \\ &\quad \left. + \frac{\beta^2 d}{4(d+4)^2 L_1(g)} \delta^2 + \frac{1}{N+1} \sum_{k=0}^N E_{\mathcal{U}_k} (\|\nabla g_\beta(\boldsymbol{\theta}_k)\|) \delta^2 \right]. \end{aligned} \quad (24)$$

Clearly, $\frac{1}{N+1} \sum_{k=0}^N E_{\mathcal{U}_k} (\|\nabla g_\beta(\boldsymbol{\theta}_k)\|) \leq \delta^2$.

Since $\vartheta_k^2 = E_{\mathcal{U}_k} (\|\nabla g(\boldsymbol{\theta}_k)\|^2) \leq 2E_{\mathcal{U}_k} (\|\nabla g_\beta(\boldsymbol{\theta}_k)\|^2) + \frac{\beta^2(d+4)^2}{2} L_1^2(g)$, ϑ_k^2 is in the same order as $E_{\mathcal{U}_k} (\|\nabla g_\beta(\boldsymbol{\theta}_k)\|^2)$.

In order to satisfy $\frac{1}{N+1} \sum_{k=0}^N \vartheta_k^2 \leq \delta^2$, we need to choose $\beta \leq O(\frac{\delta}{dL_1(g)})$, then N is bounded by $O(\frac{d}{\delta^2})$.